Reprograming gene expression in hibernating *C. elegans* involves the IRE-1/XBP-1 pathway.

AUTHORS LIST:

Melanie L. Engelfriet [1], Yanwu Guo [1], Andreas Arnold [2, 3], Eivind Valen [1], and Rafal Ciosk [1]*

AFFILIATIONS:

[1] Section for Biochemistry and Molecular Biology, Department of Biosciences, University of Oslo, Oslo, Norway

[2] Division of Molecular Neuroscience, Department of Biomedicine, University of Basel, Basel, Switzerland

[3] University Psychiatric Clinics, University of Basel, Basel, Switzerland

* Correspondence and request for materials should be addressed to R.C. (email: rafal.ciosk@ibv.uio.no)

Keywords:

Hypothermia, hibernation, cold, global translation, fatty acid desaturation, ER stress, UPR, IRE-1, XBP-1, LIPS-11

ABSTRACT

In the wild, many animals respond to cold temperatures by entering hibernation. In the clinic, controlled cooling is used in transplantation and emergency medicine. Yet, the molecular mechanisms that the cells use to survive cold remain largely unexplored. One aspect of cold adaptation is a global downregulation of protein synthesis. Studying it in the nematode *Caenorhabditis elegans*, we find that the translation of most mRNAs continues in the cold, albeit at a slower rate, and propose that cold-specific gene expression is regulated primarily at the transcription level. Moreover, we show that the transcription of some cold-induced genes reflects the activation of unfolded protein response (UPR) mediated by the conserved IRE-1/XBP-1 signaling pathway. Our results suggest that the activation of this pathway stems from cold-induced perturbations in proteins and lipids in the endoplasmic reticulum and that its activation is beneficial for cold survival.

INTRODUCTION

One constant facet of hibernation appears to be the global reduction of protein synthesis. It is manifested, among others, by the loss of polyribosomes (aka polysomes associated with robust translation) and the inhibition of basic translation factors like eIF2α and eEF2 that are required for the initiation and elongation steps of translation, respectively (Chen et al., 2001; Frerichs et al., 1998; Knight et al., 2000; Van Breukelen and Martin, 2001). Cells from non-hibernating species, including humans, also respond to cold by downregulating translation (Hofmann et al., 2012). At the same time, numerous studies highlight the importance of cold-induced gene expression, raising questions about the mechanism facilitating the expression of specific genes against the overall reduction of protein synthesis.

Hibernation has been traditionally studied in non-standard animal models like squirrels, bats, or bears. Nonetheless, simple genetic models are often advantageous in dissecting complex biological phenomena. Thus, to better understand gene expression underlying cold adaptation, we employ the nematode *C. elegans*: a rapid, morphologically simple, and genetically tractable animal model. These animals thrive in temperate climates, indicating that, in the wild, they can tolerate spells of cold (Frezal and Felix, 2015). In a laboratory, deep cooling of *C. elegans* either leads to death (when the cooling is rapid) (Habacher et al., 2016; Ohta et al., 2014; Robinson and Powell, 2016) or to a dormant hibernation-like state (when the cooling is gradual) (Habacher et al., 2016; Ohta et al., 2014). During "hibernation" *C. elegans* suppresses aging (Habacher et al., 2016). Although this response and mammalian hibernation are not equivalent, some aspects appear to be conserved (Pekec et al., 2022). Thus, the advantages of a simple genetic model may be useful in uncovering conserved aspects of cellular adaptations to cold.

Here, we demonstrate that *C. elegans*, like hibernating animals, respond to cold by globally reducing mRNA translation. Overall, the translation of individual transcripts

correlates with their levels, suggesting that cold-specific gene expression is regulated primarily through transcription. We validated this hypothesis by focusing on one up-regulated gene, *lips-11*, which encodes a putative lipase implicated in unfolded protein response (UPR) (Shen et al., 2005). The UPR consists of three stress-sensing and transducing branches: IRE1, PEK1, and ATF6, all conserved in *C. elegans* (Hetz et al., 2020). Once activated, the UPR restores homeostasis by various means, including by remodeling transcription and translation. We find that, in *C. elegans*, cold activates the IRE-1 branch of the UPR. While IRE-1 signaling is induced typically in response to protein misfolding, we present evidence that, in the cold, the IRE1 pathway responds to both protein and lipid bilayer stress in the endoplasmic reticulum (ER) and that its activation is beneficial for hibernating animals.

RESULTS

Protein synthesis is globally reduced in hibernating *C. elegans.*

In several species and cultured cells, cooling leads to a global reduction of translation (Chen et al., 2001; Frerichs et al., 1998; Hofmann et al., 2012; Knight et al., 2000; Van Breukelen and Martin, 2001). To test if this occurs in *C. elegans*, we used a previously described cooling paradigm and sampling across different temperatures and time points (**Figure 1A**). We combined this with either polysome profiling or SUrface SEnsing of Translation (SUnSET). The former method separates translated mRNAs according to the number of bound ribosomes. The latter involves the incorporation of puromycin into newly synthesized peptides and subsequent detection of the incorporated puromycin by western blotting (Arnold et al., 2014; Schmidt et al., 2009). By polysome profiling, we observed in the cold a massive loss of polyribosomes (multiple ribosomes associated with mRNAs), with a concomitant increase in monosomes (**Figure 1B**). By SUnSET, we observed a stark drop in puromycin incorporation in hibernating animals (**Figure 1C**). Thus, consistent with observations in other species, severe cooling is accompanied in *C. elegans* by a global reduction of protein synthesis.

Transcription is a major determinant of cold-specific gene expression.

Although global translation decreases in the cold, the translation of specific transcripts still could be regulated, i.e., activated or repressed. To examine this possibility, we combined ribosomal profiling with total RNA sequencing across different temperatures and time points (**Supplementary files 1 and 2**). We made several observations. First, while shifting animals from 20°C to 10°C had a relatively mild impact on translation (ribosomal occupancy), the subsequent shift from 10°C to 4°C had a strong effect. Then, continuing the incubation at 4°C again had a relatively small effect (**Figure 2A** and **Figure 2A – figure supplement 1**). Thus, most translational remodeling occurs during the first day of incubation at 4°C. Focusing on this

transition (10°C to 4°C day 1), we observed a good correlation between mRNA levels and translation (**Figure 2A**). Thus, although general protein synthesis is reduced in the cold, the available mRNAs appear to be translated. However, we did observe some exceptions, such as a group of transcripts whose translation appeared reduced with no concomitant drop in mRNA levels (red dots in **Figure 2A**), suggesting the existence of dedicated repressive mechanism(s). Intriguingly, this group includes mRNAs encoding three fatty acid desaturases (FAT-2, -3, and -4; **Supplementary file 3**). This finding is surprising, because desaturation of membrane lipids has been thought to play an important role in cold adaptation (Hayward et al., 2007).

For most transcripts, however, their translation correlates with their levels. In other words, the abundance of a particular protein appears to depend primarily on the abundance of its mRNA. Since transcription is the main determinant of mRNA levels, these results suggest that cold-specific gene expression primarily depends on transcription activation. To test this, we selected one gene, *lips-11*, whose expression increased the most during the shift from 10°C to 4°C (green dot in **Figure 2A**). To test if cold induces *lips-11* transcription, we generated a strain expressing a GFP reporter, whose expression depends on the endogenous *lips-11* promoter (P*lips-11*) and the *unc-54* 3'UTR (permitting unregulated expression of the attached open reading frame). We observed that the *lips-11* promoter was sufficient to induce GFP expression in the cold (**Figure 2B**). Thus, while we cannot exclude that cold additionally impacts the stability of some mRNAs, we propose that cold-specific gene expression is shaped mainly at the transcription level.

Cold-induced transcription of *lips-11* depends on the IRE-1/XBP-1 branch of the UPR.

Intriguingly, *lips-11* belongs to genes activated by the UPR during ER stress (UPR^{ER}) (Shen et al., 2005). Indeed, we observed that the P*lips-11* GFP reporter's levels increased upon treating animals with the protein glycosylation inhibitor tunicamycin, a UPR^{ER} inducer (**Figure 3 –**

figure supplement 1). This observation prompted us to examine if the induction of *lips-11* in the cold depends on a particular branch of the UPR^{ER} signaling; IRE-1, ATF-6, or PEK-1. Indeed, we observed reduced levels of the *lips-11* reporter upon RNAi-mediated depletion of *ire-1*, but not *atf-6* or *pek-1* (**Figure 3A**). Thus, *lips-11* expression in the cold depends on the UPR^{ER} signal transducer IRE-1.

In response to ER stress, the endoribonuclease domain of IRE-1 is activated and promotes the processing of *xbp-1* mRNA, which gives rise to the functional form of the XBP-1 transcription factor. As XBP-1-independent functions of IRE-1 have been reported, we first examined if *xbp-1* mRNA is processed in the cold. To do this, we used a published *xbp-1* splicing reporter strain, wherein the *xbp-1* promoter drives the expression of genomic *xbp-1* fused to GFP, which is expressed in frame upon processing by activated IRE-1 (Ozbey et al., 2020). Importantly, we observed a significant upregulation of XBP-1::GFP in the cold (**Figure 3B**), indicating the activation of the IRE-1/XBP-1 branch of the UPR^{ER}. Moreover, in addition to IRE-1, the cold-induced expression of the *lips-11* reporter also depended on XBP-1 (**Figure 3C**). Thus, the upregulation of *lips-11* in hibernating *C. elegans* depends on the IRE-1/XBP-1 branch of the UPR^{ER}.

Hibernation specifically activates the IRE-1 branch of the UPR^{ER}.

The activation of IRE-1 in the cold suggests that hibernating animals experience ER stress. To confirm this, we utilized a commonly used UPR^{ER} reporter strain, wherein GFP expression is driven by the promoter of *hsp-4*, the *C. elegans* homolog of the ER chaperone BiP (Calfon et al., 2002). Indeed, the expression of this reporter gradually increased in the cold (**Figure 4A**). By following the expression of mitochondrial chaperones *hsp-6* (homolog of HSP70) and *hsp-60* (homolog of HSP60), we additionally examined if cold elicits UPR in the mitochondria (UPR^{mito}) (Yoneda et al., 2004). However, by contrast to *hsp-4*, neither *hsp-6* nor *hsp-60* were

induced in the cold (**Figure 4A – figure supplement 1**). Thus, hibernating animals appear to experience stress in the ER but not mitochondria.

While we showed that *lips-11* upregulation is mediated by the IRE-1/XBP-1 pathway, other branches of the UPR^{ER} could be activated in the cold. Testing this possibility, we examined the expression of select UPR^{ER} target genes regulated through the IRE-1 (*dnj-27*, *srp-7*, *C36B7.6*), the ATF-6 (*cht-1*, *ZC168.2*), or the PEK-1 (*cbp-3*, *R02D3.8*) pathway (Shen et al., 2005). While the levels of these transcripts did not change significantly after one day in the cold (**Figure 4B – figure supplement 1**), four transcripts were more abundant after three days (**Figure 4B**). Notably, 3/4 of them are known targets of the IRE-1 pathway. Although a more comprehensive analysis is needed to reach firm conclusions, these findings suggest that cold triggers the UPR^{ER} primarily via the activation of IRE-1.

The cold-induced UPR^{ER} stems from both protein misfolding and lipid disequilibrium.

ER stress and subsequent activation of the UPR^{ER} are typically associated with misfolded proteins accumulating in the ER lumen. To test if cold aggravates protein misfolding, we employed another reporter strain, wherein YFP is fused to a mutated form of the *C. elegans* cathepsin L-like protease ($CPL\text{-}1^{W32A,Y35A}$), which does not fold properly and accumulates during ER stress (Efstathiou et al., 2022). We found that the levels of misfolded CPL-1 modestly increased after one day in the cold but then returned to basal levels after a longer cold exposure (**Figure 5**). Thus, disturbed ER proteostasis could, at least transiently, trigger the activation of UPR^{ER} in hibernating animals.

Apart from protein misfolding, lipid disequilibrium is also known to trigger UPR^{ER} (Halbleib et al., 2017; Tam et al., 2018; Volmer et al., 2013). The IRE-1 pathway is specifically activated when the ratio between phosphatidylcholine (PC) and phosphatidylethanolamine (PE) decreases, or when the levels of unsaturated fatty acids become insufficient (Ariyama et

al., 2010; Hou et al., 2014; Thibault et al., 2012). In the latter case, reduced content of unsaturated fatty acids (FAs) results in a decreased ER membrane fluidity, which is thought to increase the oligomerization and thus the activation of IRE-1 (Halbleib et al., 2017). So, we asked next if dietary supplementation of unsaturated FAs or choline (crucial for PC synthesis) impacts the IRE-1-dependent induction of the *lips-11* reporter in the cold. We found that supplementing the diet with either saturated (palmitic acid) or unsaturated FAs (oleic acid or linoleic acid) did not prevent the expression of the *lips-11* reporter (**Figure 6 – figure supplement 1**; if anything, adding oleic acid appeared to upregulate the reporter). While these experiments have certain caveats (for example it is impossible to precisely control the concentration of internalized FAs), they suggest that insufficient lipid desaturation is not the main trigger of UPR^{ER} in the cold. By contrast, the dietary supplementation of choline led to reduced expression of *lips-11* and *hsp-4* reporters in hibernating animals (**Figure 6A and Figure 6B**, respectively). Together, these experiments suggest that cold-induced activation of UPR^{ER} could be triggered by sensing disruptions in both protein and lipid homeostasis, with the latter related to insufficient levels of PC rather than unsaturated FAs.

IRE-1-dependent signaling is important for cold survival.

Cold triggers the IRE-1/XBP-1 signaling pathway, but for what purpose? If it helps animals in cold adaptation, then inhibiting this pathway may be expected to impair cold survival. At standard temperature, the loss-of-function *ire-1(ok799)* mutants display no obvious defects. In the cold, however, we observed that these mutants survived less well than the wild type (**Figure 7A**). Thus, IRE-1/XBP-1 signaling appears to improve cold survival, presumably by activating its downstream target(s). A natural candidate is LIPS-11, but we found that its RNAi-mediated depletion had no obvious impact on cold survival. Assuming that the RNAi was effective, it suggests that either LIPS-11 plays no role in cold survival, or it functions redundantly with

other IRE-1/XBP-1 targets. Several previous studies reported IRE-1-dependent genes activated in response to protein misfolding (UPR^{PT}; (Shen et al., 2005), lipid bilayer stress (UPR^{LBS}; (Koh et al., 2018), or cold when using different cooling conditions (Dudkevich et al., 2022). To examine if these genes are also activated by cold treatment in this study, we extracted them from the publications (**Supplementary file 4**) and examined their overlap with the cold-induced transcripts from **Figure 2A**. Curiously, we observed relatively little overlap between the different gene sets (**Figure 7 – figure supplement 1**). While the UPR^{PT} and the UPR^{LBS} are known to regulate largely distinct targets (Koh et al., 2018), this analysis further suggests than IRE-1-mediated gene activation is largely context-dependent. Also, since many cold-induced genes from this study appear to be unrelated to the examined IRE-1 gene sets, we hypothesize that additional pathways(s) work alongside the IRE1/XBP-1 pathway to shape gene expression in the cold.

Summarizing our findings in a model (**Figure 7B**), cold-induced protein and lipid stress in the ER specifically induces the IRE-1 branch of the UPR. Following the IRE-1-mediated processing of *xbp-1* mRNA, the XBP-1 transcription factor enters the nucleus and activates its target genes. These include *lips-11*, but the regulation of additional targets is necessary to explain the beneficial effect of IRE-1 on cold survival.

DISCUSSION

Our findings indicate that *C. elegans* respond to severe cold by decreasing protein synthesis, consistent with observations in other models. Since translation is one of the most energy-consuming biological processes, its global reduction will help preserve cellular energy stores. In poikilotherms (animals whose body temperature depends on the environment), reducing global translation is part of their physiological response to cold. A similar situation occurs in homeotherms (animals whose temperature depends on metabolism) who are capable of temporal heterothermy, i.e., can change their body temperature in a circadian or seasonal circle. In other homeotherms (like humans), the global reduction of protein synthesis may help survive accidental hypothermia or repair peripheral cold injuries affecting the extremities and exposed skin.

Despite the general reduction of protein synthesis in the cold, most mRNAs continue to be translated, albeit at a lower rate. Consequently, either transcription or mRNA stability could regulate cold-specific gene expression. We present evidence that the expression of some cold-inducible genes depends on the transcription factor XBP-1, which functions downstream from IRE-1. Curiously, another cooling procedure (involving shifting animals from 15°C to 2°C) was reported to elicit IRE-1 signaling independently from XBP-1. In that case, IRE-1 activation occurs in neurons, but it stimulates the remodeling of lipid metabolism in other tissues (Dudkevich et al., 2022). In that context, IRE-1 was proposed to adjust the balance between saturated and unsaturated FAs, because supplementing the diet with unsaturated FAs could bypass the requirement for IRE-1. By contrast, the IRE-1 signaling reported here depends on XBP-1, and the dietary supplementation of non-saturated FAs did not prevent the activation of IRE-1/XBP-1 signaling. This observation is consistent with a previous study, which showed that inhibiting *C. elegans* fatty acid desaturases has relatively little impact on *C. elegans* tolerance of severe cold (Murray et al., 2007). Combined with our observation that some FA

desaturases are translationally repressed in the cold, these findings collectively suggest that desaturated FAs are not limiting in hibernating *C. elegans*, although the situation appears to be different when these animals are cultured at low but physiologically tolerable temperatures (Svensk et al., 2013). Summarizing, cold seems to activate IRE-1-mediated signaling in various ways and with different outcomes, possibly influenced by the animal's physiological state and specific cooling conditions.

What triggers the activation of the IRE-1/XBP-1 pathway in the cold? Using the CPL-1$^{W32A, Y35A}$ protein folding sensor, we observed a transient misfolding (present at day 1, but not 3 in the cold). Since protein synthesis is strongly downregulated in the cold, the burden of misfolded proteins may decrease over time, suggesting that additional cues evoke UPR^{ER} at later stages of hibernation. Intriguingly, the dietary supplementation of choline reduced IRE-1-dependent expression during both early and later stages of hibernation, suggesting that alterations involving one or more choline derivatives may contribute to ER stress. Since choline is essential for PC synthesis (a critical component of biological membranes (Akkers et al., 2010)), the IRE-1 pathway may monitor a PC-sensitive aspect of ER biology. For example, it could detect alterations in transmembrane channels or peripheral membrane-binding proteins, whose activities depend on the physical properties of membrane lipids (Allende et al., 2004; Janmey and Kinnunen, 2006).

Finally, while the activation of IRE-1-dependent signaling appears to be an important aspect of *C. elegans* responses to cold, is it also used in other animals? There is emerging evidence suggesting that it could be so. In culture, human neurons exposed to moderate hypothermia activate the ER stress response and induce all three branches of the UPR, including the IRE1 (Rzechorzek et al., 2016). Whether this holds *in vivo* and applies to deep hypothermia remains to be tested. Nonetheless, the same study suggested that cooling-induced UPR^{ER} may be neuroprotective, potentially helping understand the cellular

mechanisms underlying the therapeutic benefits of hypothermia. In the clinic, organ cooling is used in transplantation, and therapeutic hypothermia is applied, among others, in stroke or trauma, helping preserve the functions of key organs like the brain or heart (Kutcher et al., 2016; Yenari and Han, 2012). Therefore, understanding how cold elicits UPR^{ER} may help in discovering interventions mimicking the beneficial effects of cold, but at a thermoneutral temperature. Such preconditioning could be administered to individuals at risk of accidental hypothermia or patients undergoing therapeutic hypothermia, aimed at minimizing potential injuries and enhancing recovery.

METHODS

C. elegans strains and maintenance

Unless stated otherwise, animals were maintained as previously described, grown at 20°C on 2% Nematode Growth Media (NGM) agar plates, seeded with the *E. coli* OP50 bacteria. All strains used in this study are listed in **Supplementary file 5A**. Synchronized animals were obtained by extracting embryos from gravid adults with a bleaching solution (30% (v/v) sodium hypochlorite (5% chlorine) reagent (ThermoFisher Scientific; 419550010), 750 mM KOH). The embryos were left to hatch in the absence of food into arrested L1 larvae by overnight incubation at room temperature in M9 buffer (42 mM Na2HPO4, 22 mM KH2PO4, 86 mM NaCl, 1 mM MgSO4).

Cold adaptation

Synchronized L1 larvae were grown at 20°C until reaching the 1-day-old adult stage. Animals were adapted to the cold for 2 hours at 10°C before being transferred to 4°C.

Polysome and ribosome profiling

Polysome profiling and ribosome profiling were performed as previously described (Arnold et al., 2014; Scheckel et al., 2012).

Computational processing of RNA-seq and ribosome profiling

Both RNA-seq and ribosome profiling were processed with the ribo-seq pipeline in ORFik (v1.22.2). The pipeline was run with default parameters and wraps several steps: stripping adapters using fastp (v0.23.4) using the adapter sequence "TGGAATTCTCGGGTGCCAAGG", mapping reads with STAR (v2.7.11b) and expression

(FPKM) estimates using DESeq2(v1.42.1). The code for this pipeline can be found at https://www.bioconductor.org/packages/release/bioc/vignettes/ORFik/inst/doc/Ribo-seq_pipeline.html.

Western blot analysis

Animals were harvested from plates, washed thrice in M9 buffer and pelleted before being snap-frozen in liquid nitrogen. Protein extracts were prepared by grinding the pellet with a mortar and pestle in the presence of liquid nitrogen and dissolving in Lysis Buffer (50 mM HEPES (pH 7.4), 150 mM KCl, 5 mM MgCl2, 0.1% Triton X-100, 5% glycerol (w/vol), 1 mM PMSF, 7 mg/ml cOmplete Proteinase Inhibitor Tablets (Roche, 11697498001)). Debris was removed by centrifugation at 16,100 x g for 20 minutes at 4°C. Protein concentrations were measured by Bradford Assay (Bio-Rad). The required amount of 4x NuPAGE™ LDS Sample Buffer (Invitrogen, NP0007) and 10x NuPAGE Sample Reducing Agent (Invitrogen, NP0004) was added to the protein samples, followed by an incubation at 70°C for 10 minutes. Proteins were separated by SDS-PAGE and transferred onto a polyvinylidene difluoride membrane by wet-transfer. Membranes were washed thrice for 5 minutes with PBS-T, blocked for 1 hour in Intercept (TBS) Blocking Buffer (LI-COR, 927-60001), and incubated overnight at 4°C with primary antibodies diluted in the same blocking buffer. The following primary antibodies were used: 1:10,000 monoclonal mouse anti-puromycin (Merck, MABE343), and 1:5,000 polyclonal rabbit anti-actin (Abcam, ab8227). Detection was carried out with IRDye 680RD-conjugated goat anti-mouse secondary antibody (LI-COR Biosciences, 926-68070) or IRDye 800CW-conjugated goat anti-rabbit secondary antibody (LI-COR Biosciences, 926-32211) and infrared imaging (LI-COR Biosciences, Odyssey CLx).

SUnSET assay

A total of 12,000 synchronized L1 larvae were grown at 20°C and adapted to the cold as described earlier or kept at 20°C. Animals were cultivated for 1 or 3 additional days at 4°C or 20°C. The SUnSET assay was carried out essentially as previously described (Arnold et al., 2014), with modifications to assay protein synthesis at 4°C. In brief, animals were washed twice in S-basal, resuspended in 4 ml S-medium, and transferred to a 50 ml Erlenmeyer. An overnight culture of *E. coli* OP50 was 10x concentrated in S-medium and 750 µl was added to the animals together with 250 µl of 10 mg/ml puromycin (Millipore Sigma, P8833). The animals were grown for 4 hours at 200 rpm before harvesting. Animals were washed thrice with S-basal, pelleted, and snap frozen in liquid nitrogen. Lysates were prepared as described in the western blot procedures and 40 µg of total protein was loaded per well. The incorporation of puromycin into nascent peptides was measured by normalizing band intensities from anti-puromycin to anti-actin antibodies.

Construction of the *lips-11::GFP* reporter strain

The P*lips-11::GFP::unc-54* 3'UTR construct was generated via the MultiSite Gateway Technology (Thermo Fisher Scientific, 12537-023). The *lips-11* promoter (1140 bp) and GFP (867 bp) were amplified from *C. elegans* genomic DNA and a plasmid carrying GFP::H2B (pCM1.35) (Merritt et al., 2008), before being inserted into the entry vectors pDONRP4P1R and pDONR221, respectively (oligos are listed in **Supplementary file 5B**). The resulting entry vectors were recombined along with the entry vector pCM5.37, carrying the *unc-54* 3'UTR (699 bp) (Merritt et al., 2008), and the destination vector pCFJ150 (Frokjaer-Jensen et al., 2008), carrying chromosome II integration sites together with the *unc-119* (+) gene, resulting in the expression clone P*lips-11::GFP::unc-54* 3'UTR. Transgenic animals were obtained via single-copy integration into the *ttTi5605* locus on chromosome II by injecting EG4322

(*ttTi5605 II; unc-119(ed3) III*) animals with the expression clone (Frokjaer-Jensen et al., 2008).

Microscopy

Animals were grown and adapted to the cold as described or kept at 20°C. Reporter strains were imaged after an additional 1 or 3 days at 20°C or 4°C. Animals were anesthetized in a drop of 5 mM levamisole in M9 buffer on a 2% (w/v) agarose pad, clustered, covered with a cover slip and immediately imaged with the Zeiss AxioImager Z1 microscope. Micrographs were acquired with an Axiocam MRm REV2 CCD camera using the Zen software (Zeiss) and processed with Image J. The specific area that was analyzed for fluorescent intensities, as well as the number of measurements, is indicated in each figure legend.

Induction of ER stress by tunicamycin treatment

Animals were grown at 20°C on NGM agar plates seeded with *E. coli* OP50. At the 2 day-old adult stage, animals were shifted to plates containing 20 µg/ml tunicamycin (Millipore Sigma, T7765), prepared from a 1 mg/ml stock solution dissolved in DMSO. Animals were grown for 6 hours at 20°C in the presence of tunicamycin. Control animals were treated similarly on plates containing the same volume of DMSO.

Generation of iOP50 RNAi bacteria

Plasmids targeting *ire-1*, *xbp-1*, *pek-1*, or *atf-6* were extracted from overnight cultures of *E. coli* HT115 bacteria derived from the Ahringer library using the QIAprep Spin Miniprep Kit (QIAGEN, 27104) (Kamath et al., 2003). *E. coli* OP50 bacteria were rendered RNAi competent and chemically competent as previously described (Neve et al., 2020). The resulting iOP50

bacteria were transfected with 1 µl of the purified plasmids derived from the Ahringer library for downstream gene-specific RNAi or with the plasmid vector L4440 for mock RNAi (Fire et al., 1998; Kamath et al., 2003).

RNAi

Gene-specific knockdown was achieved by feeding the animals with bacteria carrying plasmids expressing double-stranded RNA, sourced from either the Vidal or Ahringer libraries (Kamath et al., 2003; Rual et al., 2004). Overnight cultures of *E. coli* HT115 (for RNAi at 20°C) or *E. coli* iOP50 bacteria (for RNAi at 4°C) were induced for 1 hour with 1 mM IPTG and seeded on NGM agar plates containing 1 mM IPTG and 50 µg/ml carbenicillin. Synchronized L1 larvae were grown on the RNAi-inducing agar plates at 20°C until reaching the 1 day-old adult stage and were either adapted to the cold as described and kept for 1 or 3 days at 4°C or kept at 20°C for the same duration. Bacteria containing the 'empty' L4440 vector were utilized as a mock RNAi control for all experiments.

Dietary supplementation

For choline supplementation assays, a working stock of 200 mg/ml choline (Millipore Sigma, C7527) in water was added to autoclaved NGM media at 55°C to a final concentration of 50 mM. Fatty acid supplemented plates were prepared as previously described with adaptations (Deline et al., 2013). In brief, working stocks of 100 mM were prepared by dissolving palmatic acid (Millipore Sigma, P9767), oleic acid (Millipore Sigma, O7501), and linoleic acid (Millipore Sigma, L8134) in 50% ethanol. Fatty acid sodium salts were added to autoclaved NGM medium containing 0.1% Tergitol (NP40) to a final concentration of 0.8 mM. Fatty acid

supplemented plates were covered with foil to prevent light oxidation. All plates were seeded with an overnight culture of *E. coli* OP50 and dried for 3 days before use.

The assay for *C. elegans* cold survival

Cold survival experiments were performed as previously described (Pekec et al., 2022). In brief, a minimum of 150 synchronized L1 larvae were grown and adapted to the cold as previously described for each time point. Animals were sampled at the indicated time points and their survival was scored after recovery for 24 hours at 20°C, animals that were unresponsive to touch were considered dead. Cold survival was assessed from six independent biological replicates, with a minimum of 850 animals used to assess the viability at each indicated time point.

RT-qPCR

Approximately 6,000 animals that were adapted to the cold and kept for 1 or 3 days at 4°C or kept at 20°C for the same time were subjected to RNA extraction as previously described (Arnold et al., 2014). Subsequently, genomic DNA was removed by DNase treatment and the quality of the RNA was assessed using the NanoDrop Spectrophotometer. Reverse transcription was performed by using the SuperScript™ IV First – Strand Synthesis System with random primers, following the protocol from the suppliers. RT-qPCR was performed with 2.5 µl of 1:5 diluted cDNA, 0.25 µl of 10 µM gene-specific primers (**Supplementary file 2, Table 3**) and 2 µl of the HOT FIREPol EvaGreen qPCR Mix (Solis BioDyne, 08-36-00001) in a LightCycler 96 qPCR machine.

Data availability

RNA sequencing information from this research can be found in the GEO repository under the following accession numbers: GSE269587 (RNA-seq; use the reviewer token mdkdwkiqhfeznkn) and GSE269589 (Ribo-seq; use the reviewer token gnqxucakhryhncd).

ACKNOWLEDGEMENTS

We thank Dimos Gaidatzis and the Functional Genomics and Computational Biology facilities at the Friedrich Miescher Institute for Biomedical Research for the initial genomic analysis. We also thank Agnieszka Chabowska-Kita and the Laboratory of Animal Model Organisms (Institute of Bioorganic Chemistry PAS) for constructing the *lips-11* reporter strain.

ADDITIONAL INFORMATION

Funding

The research leading to these results received funding from the Norwegian Financial Mechanism 2014–2021 operated by the Polish National Science Center under the project contract nr UMO-2019/34/H/NZ3/00691. Some of the strains were provided by the CGC, which is funded by the NIH Office of Research Infrastructure Programs (P40 OD010440).

Author contributions

Melanie L. Engelfriet: Formal analysis, Investigation, Methodology, Validation, Visualization, Writing – original draft.

Yanwu Guo: Conceptualization, Formal analysis, Investigation, Methodology.

Andreas Arnold: Investigation, Formal analysis, Methodology, Validation.

Eivind Valen: Formal analysis, Visualization.

Rafal Ciosk: Conceptualization, Funding acquisition, Methodology, Project administration, Supervision, Visualization, Resources, Writing – original draft.

Declaration of interests

The authors declare no competing interests.

REFERENCES

Akkers RC, van Heeringen SJ, Manak JR, Green RD, Stunnenberg HG, Veenstra GJ (2010) **ChIP-chip designs to interrogate the genome of *Xenopus* embryos for transcription factor binding and epigenetic regulation**. *PLoS One* **5**:e8820 https://doi.org/10.1371/journal.pone.0008820

Allende D, Vidal A, McIntosh TJ (2004) **Jumping to rafts: gatekeeper role of bilayer elasticity**. *Trends Biochem Sci* **29**:325-330 https://doi.org/10.1016/j.tibs.2004.04.002

Ariyama H, Kono N, Matsuda S, Inoue T, Arai H (2010) **Decrease in membrane phospholipid unsaturation induces unfolded protein response**. *J Biol Chem* **285**:22027-22035 https://doi.org/10.1074/jbc.M110.126870

Arnold A, Rahman MM, Lee MC, Muehlhaeusser S, Katic I, Gaidatzis D, Hess D, Scheckel C, Wright JE, Stetak A, Boag PR, Ciosk R (2014) **Functional characterization of *C. elegans* Y-box-binding proteins reveals tissue-specific functions and a critical role in the formation of polysomes**. *Nucleic Acids Research* **42**:13353-13369 https://doi.org/10.1093/nar/gku1077

Calfon M, Zeng H, Urano F, Till JH, Hubbard SR, Harding HP, Clark SG, Ron D (2002) **IRE1 couples endoplasmic reticulum load to secretory capacity by processing the *XBP-1* mRNA**. *Nature* **415**:92-96

Chen Y, Matsushita M, Nairn AC, Damuni Z, Cai D, Frerichs KU, Hallenbeck JM (2001) **Mechanisms for increased levels of phosphorylation of elongation factor-2 during hibernation in ground squirrels**. *Biochemistry* **40**:11565-11570 https://doi.org/10.1021/bi010649w

Deline ML, Vrablik TL, Watts JL (2013) **Dietary supplementation of polyunsaturated fatty acids in *Caenorhabditis elegans***. *J Vis Exp* **81**:50879 https://doi.org/10.3791/50879

Dudkevich R, Koh JH, Beaudoin-Chabot C, Celik C, Lebenthal-Loinger I, Karako-Lampert S, Ahmad-Albukhari S, Thibault G, Henis-Korenblit S (2022) **Neuronal IRE-1 coordinates an organism-wide cold stress response by regulating fat metabolism**. *Cell Rep* **41**:111739 https://doi.org/10.1016/j.celrep.2022.111739

Efstathiou S, Ottens F, Schutter LS, Ravanelli S, Charmpilas N, Gutschmidt A, Le Pen J, Gehring NH, Miska EA, Boucas J, Hoppe T (2022) **ER-associated RNA silencing promotes ER quality control**. *Nat Cell Biol* **24**:1714-1725 https://doi.org/10.1038/s41556-022-01025-4

Fire A, Xu S, Montgomery MK, Kostas SA, Driver SE, Mello CC (1998) **Potent and specific genetic interference by double-stranded RNA in *Caenorhabditis elegans***. *Nature* **391**:806-811 https://doi.org/10.1038/35888

Frerichs KU, Smith CB, Brenner M, DeGracia DJ, Krause GS, Marrone L, Dever TE, Hallenbeck JM (1998) **Suppression of protein synthesis in brain during hibernation involves inhibition of protein initiation and elongation**. *Proc Natl Acad Sci U S A* **95**:14511-14516 https://doi.org/10.1073/pnas.95.24.14511

Frezal L, Felix MA (2015) **The Natural History of Model Organisms: *C. elegans* outside the Petri dish**. *Elife* **4**:e05849 https://doi.org/10.7554/eLife.05849

Frokjaer-Jensen C, Davis MW, Hopkins CE, Newman BJ, Thummel JM, Olesen SP, Grunnet M, Jorgensen EM (2008) **Single-copy insertion of transgenes in *Caenorhabditis elegans***. *Nat Genet* **40**:1375-1383 https://doi.org/10.1038/ng.248

Habacher C, Guo Y, Venz R, Kumari P, Neagu A, Gaidatzis D, Harvald EB, Faergeman NJ, Gut H, Ciosk R (2016) **Ribonuclease-Mediated Control of Body Fat**. *Dev Cell* **39**:359-369 https://doi.org/10.1016/j.devcel.2016.09.018

Halbleib K, Pesek K, Covino R, Hofbauer HF, Wunnicke D, Hanelt I, Hummer G, Ernst R (2017) **Activation of the Unfolded Protein Response by Lipid Bilayer Stress**. *Mol Cell* **67**:673-684.e8 https://doi.org/10.1016/j.molcel.2017.06.012

Hayward SA, Murray PA, Gracey AY, Cossins AR (2007) **Beyond the lipid hypothesis: mechanisms underlying phenotypic plasticity in inducible cold tolerance**. *Adv Exp Med Biol* **594**:132-142 https://doi.org/10.1007/978-0-387-39975-1_12

Hetz C, Zhang K, Kaufman RJ (2020) **Mechanisms, regulation and functions of the unfolded protein response**. *Nat Rev Mol Cell Biol* **21**:421-438 https://doi.org/10.1038/s41580-020-0250-z

Hofmann S, Cherkasova V, Bankhead P, Bukau B, Stoecklin G (2012) **Translation suppression promotes stress granule formation and cell survival in response to cold shock**. *Mol Biol Cell* **23**:3786-3800 https://doi.org/10.1091/mbc.E12-04-0296

Hou NS, Gutschmidt A, Choi DY, Pather K, Shi X, Watts JL, Hoppe T, Taubert S (2014) **Activation of the endoplasmic reticulum unfolded protein response by lipid disequilibrium without disturbed proteostasis in vivo**. *Proc Natl Acad Sci U S A* **111**:E2271-2280 https://doi.org/10.1073/pnas.1318262111

Janmey PA, Kinnunen PKJ (2006) **Biophysical properties of lipids and dynamic membranes**. *Trends in Cell Biology* **16**:538-546 https://doi.org/10.1016/j.tcb.2006.08.009

Kamath RS, Fraser AG, Dong Y, Poulin G, Durbin R, Gotta M, Kanapin A, Le Bot N, Moreno S, Sohrmann M, Welchman DP, Zipperlen P, Ahringer J (2003) **Systematic functional analysis of the *Caenorhabditis elegans* genome using RNAi**. *Nature* **421**:231-237 https://doi.org/10.1038/nature01278

Knight JE, Narus EN, Martin SL, Jacobson A, Barnes BM, Boyer BB (2000) **mRNA stability and polysome loss in hibernating Arctic ground squirrels (*Spermophilus parryii*)**. *Mol Cell Biol* **20**:6374-6379 https://doi.org/10.1128/mcb.20.17.6374-6379.2000

Koh JH, Wang L, Beaudoin-Chabot C, Thibault G (2018) **Lipid bilayer stress-activated IRE-1 modulates autophagy during endoplasmic reticulum stress**. *J Cell Sci* **131**:jcs217992 https://doi.org/10.1242/jcs.217992

Kutcher ME, Forsythe RM, Tisherman SA (2016) **Emergency preservation and resuscitation for cardiac arrest from trauma**. *Int J Surg* **33**:209-212 https://doi.org/10.1016/j.ijsu.2015.10.014

Merritt C, Rasoloson D, Ko D, Seydoux G (2008) **3' UTRs are the primary regulators of gene expression in the *C. elegans* germline**. *Curr Biol* **18**:1476-1482 https://doi.org/10.1016/j.cub.2008.08.013

Murray P, Hayward SAL, Govan GG, Gracey AY, Cossins AR (2007) **An explicit test of the phospholipid saturation hypothesis of acquired cold tolerance in *Caenorhabditis elegans***. *Proc Natl Acad Sci U S A* **104**:5489-5494 https://doi.org/10.1073/pnas.060959010

Neve IAA, Sowa JN, Lin CJ, Sivaramakrishnan P, Herman C, Ye Y, Han L, Wang MC (2020) ***Escherichia coli* Metabolite Profiling Leads to the Development of an RNA Interference Strain for *Caenorhabditis elegans***. *G3 (Bethesda)* **10**:189-198 https://doi.org/10.1534/g3.119.400741

Ohta A, Ujisawa T, Sonoda S, Kuhara A (2014) **Light and pheromone-sensing neurons regulates cold habituation through insulin signalling in *Caenorhabditis elegans***. *Nature Communications* **5**:4412 https://doi.org/10.1038/ncomms5412

Ozbey NP, Imanikia S, Krueger C, Hardege I, Morud J, Sheng M, Schafer WR, Casanueva MO, Taylor RC (2020) **Tyramine Acts Downstream of Neuronal XBP-1s to**

Coordinate Inter-tissue UPR^{ER} Activation and Behavior in *C. elegans*. *Dev Cell* **55**:754-770.e6 https://doi.org/10.1016/j.devcel.2020.10.024

Pekec T, Lewandowski J, Komur AA, Sobanska D, Guo Y, Switonska-Kurkowska K, Malecki JM, Dubey AA, Pokrzywa W, Frankowski M, Figiel M, Ciosk R (2022) **Ferritin-mediated iron detoxification promotes hypothermia survival in *Caenorhabditis elegans* and murine neurons**. *Nat Commun* **13**:4883 https://doi.org/10.1038/s41467-022-32500-z

Robinson JD, Powell JR (2016) **Long-term recovery from acute cold shock in *Caenorhabditis elegans***. *BMC Cell Biol* **17**:2 https://doi.org/10.1186/s12860-015-0079-z

Rual JF, Ceron J, Koreth J, Hao T, Nicot AS, Hirozane-Kishikawa T, Vandenhaute J, Orkin SH, Hill DE, van den Heuvel S, Vidal M (2004) **Toward improving *Caenorhabditis elegans* phenome mapping with an ORFeome-based RNAi library**. *Genome Res* **14**:2162-2168 https://doi.org/10.1101/gr.2505604

Rzechorzek NM, Connick P, Livesey MR, Borooah S, Patani R, Burr K, Story D, Wyllie DJA, Hardingham GE, Chandran S (2016) **Hypothermic Preconditioning Reverses Tau Ontogenesis in Human Cortical Neurons and is Mimicked by Protein Phosphatase 2A Inhibition**. *EBioMedicine* **3**:141-154 https://doi.org/10.1016/j.ebiom.2015.12.010

Scheckel C, Gaidatzis D, Wright JE, Ciosk R (2012) **Genome-Wide Analysis of GLD-1-Mediated mRNA Regulation Suggests a Role in mRNA Storage**. *PLoS genetics* **8**:e1002742 https://doi.org/10.1371/journal.pgen.1002742

Schmidt EK, Clavarino G, Ceppi M, Pierre P (2009) **SUnSET, a nonradioactive method to monitor protein synthesis**. *Nat Methods* **6**:275-277 https://doi.org/10.1038/nmeth.1314

Shen X, Ellis RE, Sakaki K, Kaufman RJ (2005) **Genetic interactions due to constitutive and inducible gene regulation mediated by the unfolded protein response in *C. elegans***. *PLoS Genet* **1**:e37 https://doi.org/10.1371/journal.pgen.0010037

Svensk E, Ståhlman M, Andersson CH, Johansson M, Borén J, Pilon M (2013) **PAQR-2 Regulates Fatty Acid Desaturation during Cold Adaptation in *C. elegans*.** *PLoS genetics* **9**:e1003801 https://doi.org/10.1371/journal.pgen.1003801

Tam AB, Roberts LS, Chandra V, Rivera IG, Nomura DK, Forbes DJ, Niwa M (2018) **The UPR Activator ATF6 Responds to Proteotoxic and Lipotoxic Stress by Distinct Mechanisms**. *Dev Cell* **46**:327-343.e7 https://doi.org/10.1016/j.devcel.2018.04.023

Thibault G, Shui G, Kim W, McAlister GC, Ismail N, Gygi SP, Wenk MR, Ng DT (2012) **The membrane stress response buffers lethal effects of lipid disequilibrium by reprogramming the protein homeostasis network**. *Mol Cell* **48**:16-27 https://doi.org/10.1016/j.molcel.2012.08.016

Van Breukelen F, Martin SL (2001) **Translational initiation is uncoupled from elongation at 18°C during mammalian hibernation**. *American Journal of Physiology-Regulatory Integrative and Comparative Physiology* **281**:R1374-9 https://doi.org/10.1152/ajpregu.2001.281.5.R1374

Volmer R, van der Ploeg K, Ron D (2013) **Membrane lipid saturation activates endoplasmic reticulum unfolded protein response transducers through their transmembrane domains**. *Proc Natl Acad Sci U S A* **110**:4628-4633 https://doi.org/10.1073/pnas.1217611110

Yenari MA, Han HS (2012) **Neuroprotective mechanisms of hypothermia in brain ischaemia**. *Nat Rev Neurosci* **13**:267-278 https://doi.org/10.1038/nrn3174

Yoneda T, Benedetti C, Urano F, Clark SG, Harding HP, Ron D (2004) **Compartment-specific perturbation of protein handling activates genes encoding mitochondrial chaperones**. *J Cell Sci* **117**:4055-4066 https://doi.org/10.1242/jcs.01275

FIGURES

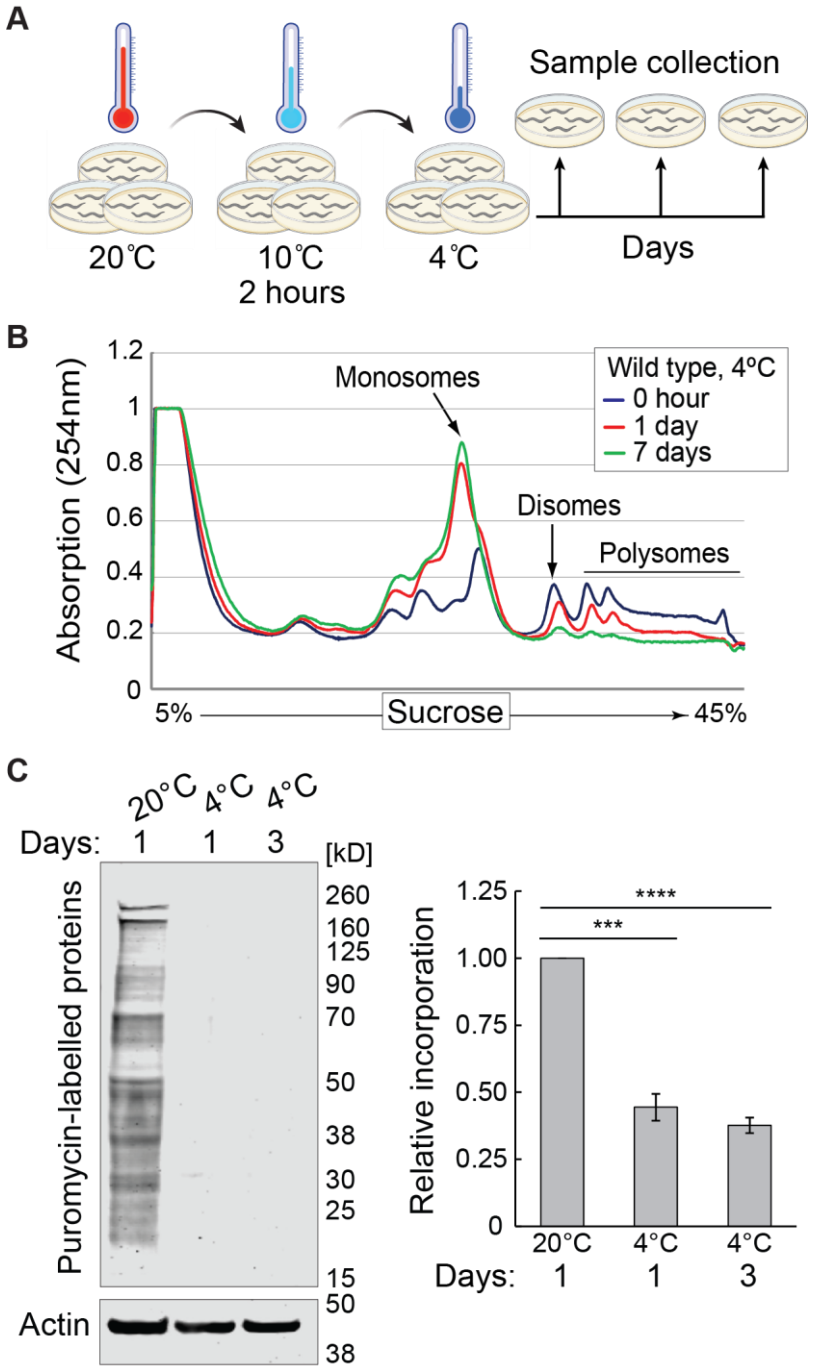

Figure 1. Global protein synthesis is suppressed in hibernating *C. elegans*.

(**A**) A schematic representation of a typical cooling experiment. One day-old adult nematodes, grown at 20°C on multiple plates, were first adapted to cold at 10°C for 2 h, and then shifted to 4°C. At indicated time points, plates were transferred back to 20°C and the animals treated in an experiment-specific manner. Created with BioRender.com. (**B**) Polysome profiles from

wild-type animals treated as shown in (A) and collected from 4°C at the indicated times. Marked are the positions of mono-, di-, and polysomes. Note a strong decrease of large polysomes with a concomitant increase of monosomes in cold, which become more pronounced with a longer cold exposure. (**C**) Protein synthesis evaluated with the SUnSET assay in animals incubated as indicated. Puromycin incorporation was detected on a western blot, with the corresponding quantification on the right. Actin (ACT-1) was used as a loading control. Error bars indicate the SEM of three biological replicates. Unpaired two-sided t-test was used for statistical analysis. ***: $p < 0.001$, ****: $p < 0.0001$.

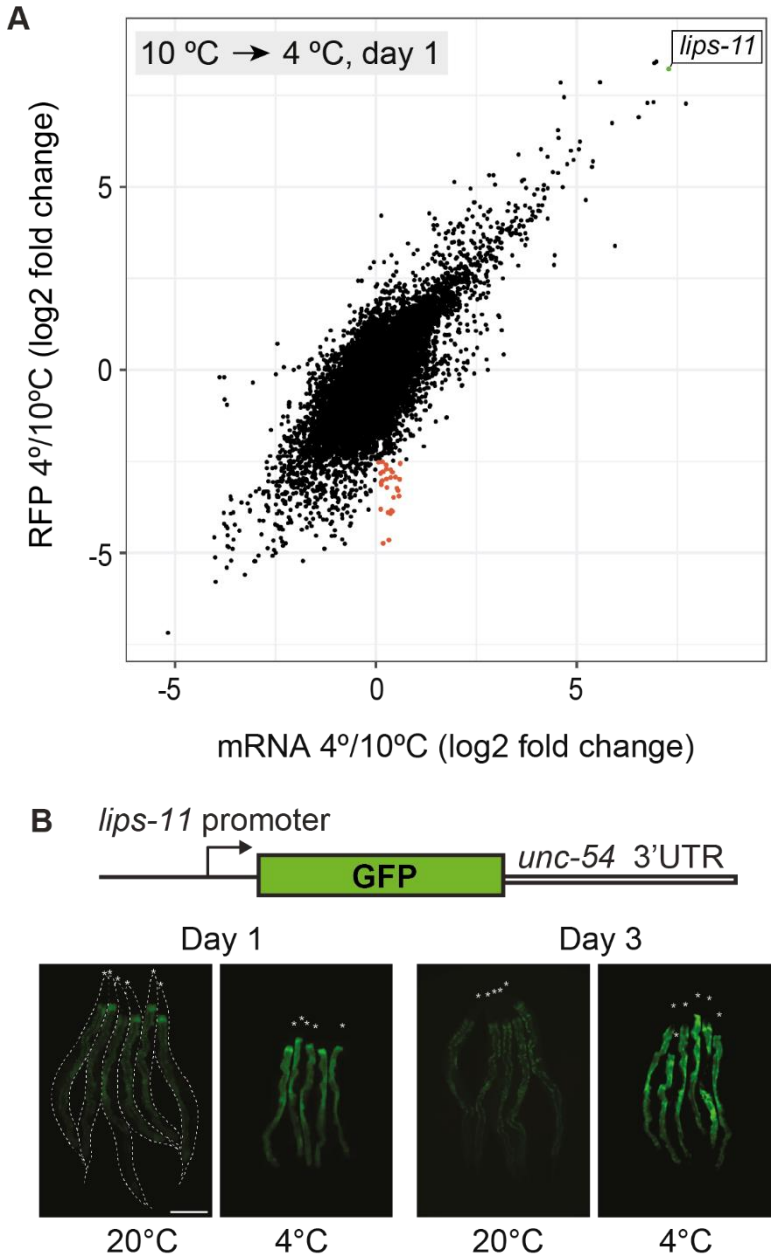

Figure 2. Transcription is the main determinant of gene expression in the cold.

(**A**) Changes in mRNA abundance (mRNA, x-axis) and translation (RPF, y-axis) for all transcripts shifting wild-type animals from 10°C to 4°C. Each dot represents the log (base 2) fold change of a single transcript. The most upregulated transcript, *lips-11*, is indicated in green. Overall, note a strong correlation between mRNA levels and translation. A small subpopulation of transcripts (red) displayed little or no change in mRNA levels but showed reduced association with ribosomes, suggesting specific translation repression. (**B**) Top:

Diagram representing a reporter construct, wherein GFP is expressed under the control of *lips-11* promoter and *unc-54* 3' UTR. Below are representative fluorescent micrographs, taken at the indicated conditions, of several bundled animals carrying the reporter GFP. The animals are outlined in the control panel and the positions of animals' heads are indicated by asterisks. The scale bar = 200 µm.

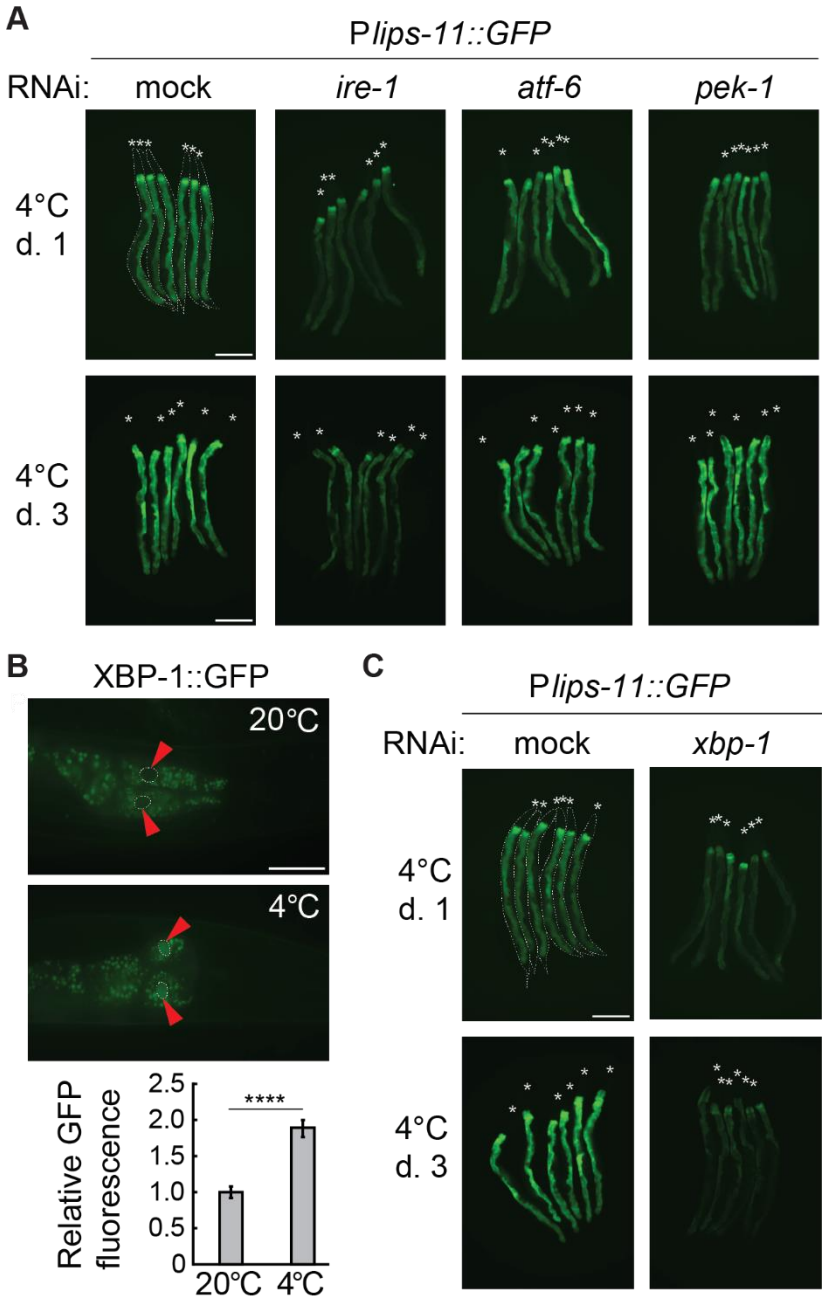

Figure 3. Transcription of *lips-11* is dependent on the IRE-1/XBP-1 pathway in the cold.

(**A**) Micrographs of several bundled animals expressing the *Plips-11::GFP* reporter, taken at the indicated conditions. Note a strong decrease in GFP reporter expression after one and three days at 4°C upon RNAi-mediated knockdown of *ire-1*, but not of *atf-6* or *pek-1*. The animals are outlined in the mock control panel and the position of the head is indicated by asterisks for all animals. The scale bar = 200 µm. (**B**) Top: Representative micrographs of adult animals expressing the *Pxbp-1::xbp-1::GFP* splicing reporter at the indicated temperatures. GFP is

expressed in frame only upon removal of the IRE-1 regulated intron in *xbp-1* mRNA. Arrowheads indicate the outlined nucleus of the most anterior pair of intestinal cells. The scale bar = 40 µm. Below: the corresponding quantification of nuclear GFP reporter expression, relative to 20°C. Between two and five nuclei were analyzed per animal, in at least fifteen animals per condition. Error bars indicate the SEM. Unpaired two-sided t-test was used for statistical analysis. ****: $p < 0.0001$. (**C**) Micrographs of mock or *xbp-1* RNAi treated *Plips-11::GFP* reporter animals, kept for one or three days at 4°C. The animals are outlined in the mock control panel and the position of the head is indicated by asterisks for all animals. The scale bar = 200 µm.

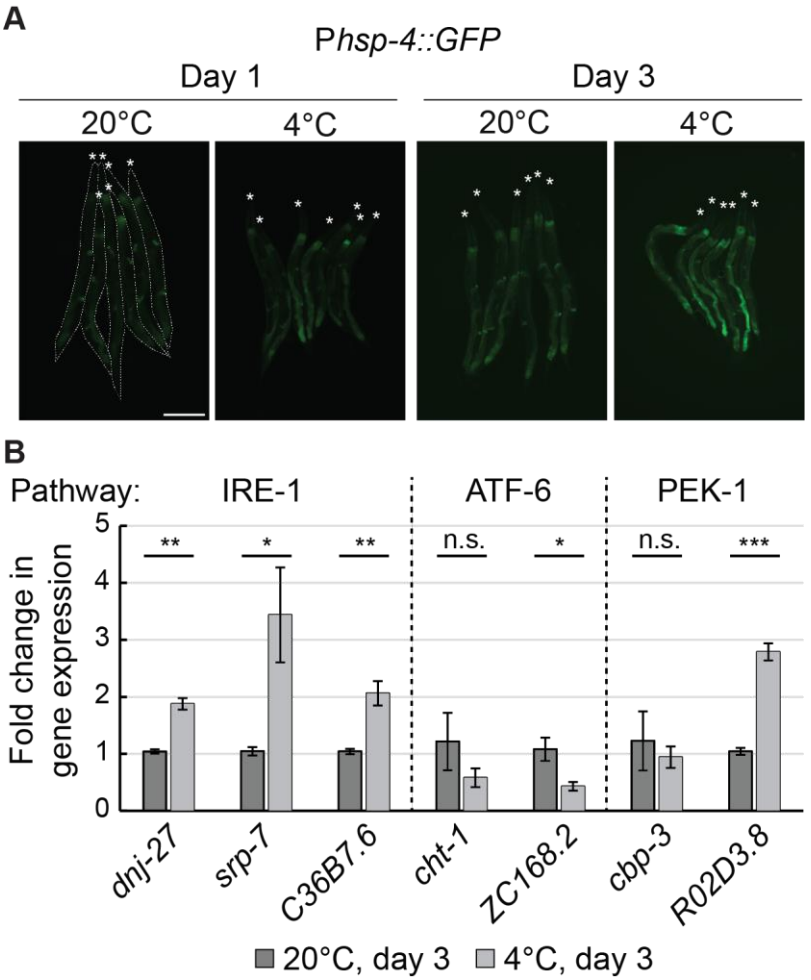

Figure 4. Cold specifically activates the UPR^{ER} through IRE-1.

(**A**) Micrographs of several bundled animals carrying the *Phsp-4::GFP* reporter, taken at the indicated temperature and time. The animals are outlined in the 20°C control panel for day 1 and the position of the head is indicated by asterisks for all animals. The scale bar = 200 µm. (**B**) RT-qPCR analysis of fold change in mRNA levels for known UPR^{ER} target genes after three days at 4°C, relative to three days at 20°C. Dashed lines separate genes that are regulated by different pathways (IRE-1, ATF-6, and PEK-1). Note that the mRNA levels of all IRE-1 responsive genes are significantly upregulated at 4°C. Error bars indicate the SEM of three biological replicates. Unpaired two-sided t-test was used for statistical analysis. ns: $p > 0.05$, *: $p < 0.05$, **: $p < 0.01$, ***: $p < 0.001$.

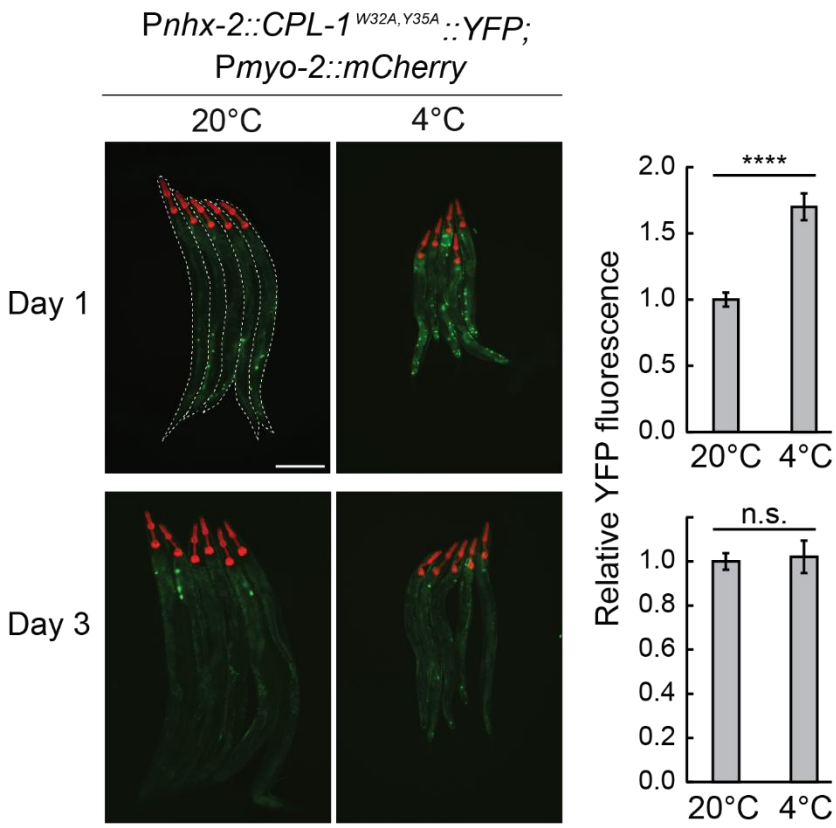

Figure 5. Misfolded protein levels increase during short-term cold exposure.

Left: representative micrographs, taken at the indicated conditions, of several bundled animals carrying the CPL-1^{W32A,Y35A}::YFP misfolding reporter. The head of each animal is indicated by pharyngeal expression of mCherry, driven by the *myo-2* promoter. Animals are outlined in the 20°C control panel for day 1. The scale bar = 200 µm. Right: the corresponding quantification of YFP fluorescence at 4°C after one or three days, relative to 20°C. YFP fluorescence was analyzed from whole animals, with a minimum of 38 animals per condition. Error bars indicate the SEM. Unpaired two-sided t-test was used for statistical analysis. ns: $p > 0.05$, ****: $p < 0.0001$.

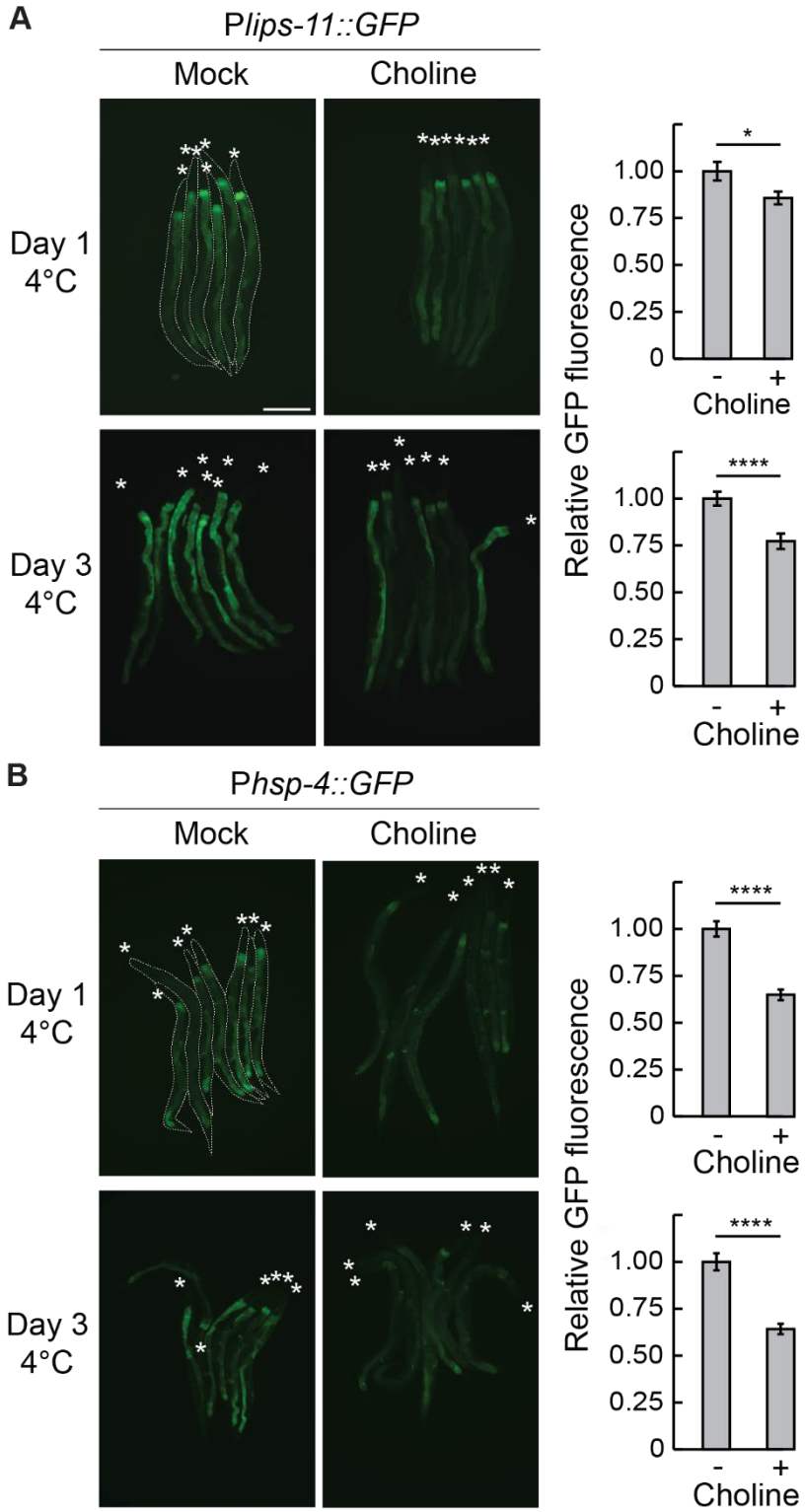

Figure 6. Choline supplementation suppresses IRE-1 regulated gene expression in the cold.

(**A**) Left: Micrographs taken after one or three days at 4°C of several bundled P*lips-11::GFP* reporter animals on a mock of 50 mM choline supplemented diet. Mock treated animals are

outlined in the 4°C control panel for day 1 and the head of all separate animals are indicated with asterisks. The scale bar = 200 µm. Right: the corresponding quantification of intestinal GFP fluorescence after one or three days at 4°C on a choline supplemented diet, relative to a mock diet. GFP fluorescence was analyzed from a minimum of 38 animals per condition. Error bars indicate the SEM. Unpaired two-sided t-test was used for statistical analysis. *: $p < 0.05$, ****: $p < 0.0001$. (**B**) Left: Micrographs taken after one or three days at 4°C of several bundled P*hsp-4::GFP* reporter animals on a mock of 50 mM choline supplemented diet. Mock treated animals are outlined in the 4°C control panel for day 1 and the head of all separate animals are indicated with asterisks. The scale bar = 200 µm. Right: the corresponding quantification of intestinal GFP fluorescence after one or three days at 4°C on a choline supplemented diet, relative to a mock diet. GFP fluorescence was analyzed from a minimum of 28 animals per condition. Error bars indicate the SEM. Unpaired two-sided t-test was used for statistical analysis. ****: $p < 0.0001$.

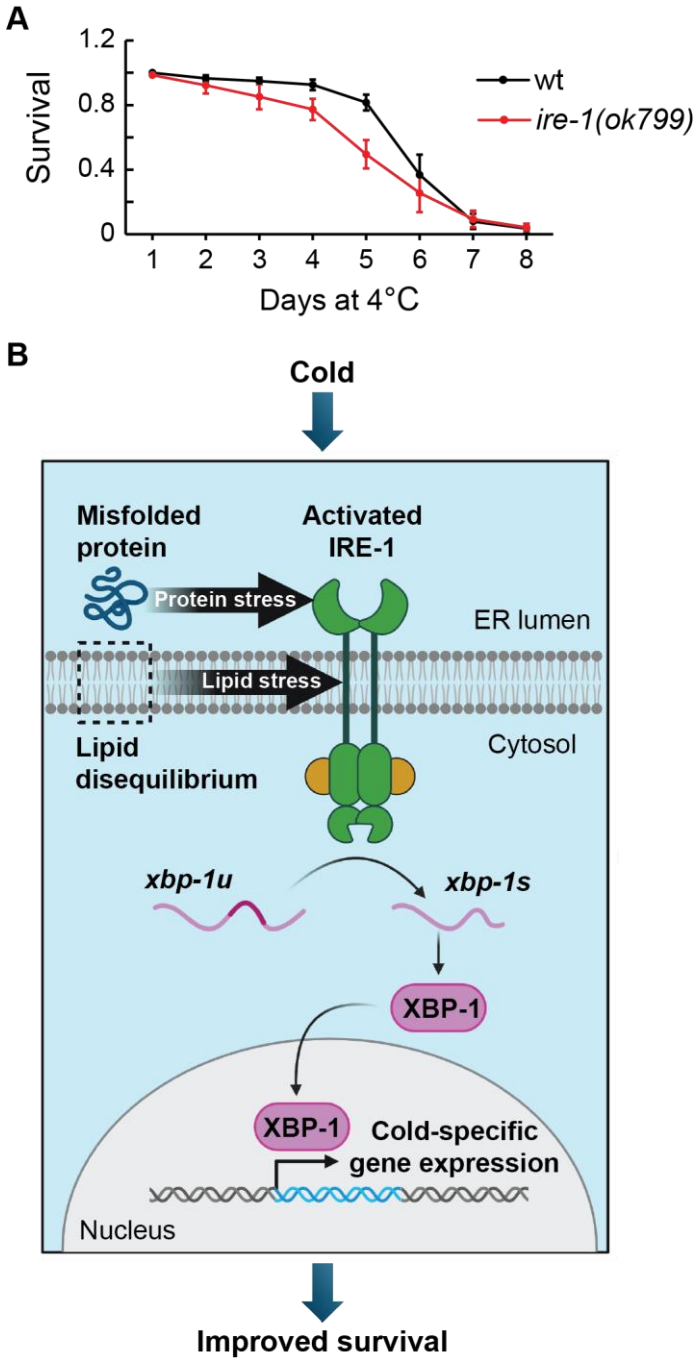

Figure 7. IRE-1 facilitates cold survival in *C. elegans* during extreme hypothermia.

(**A**) Survival curves of wild-type and *ire-1(ok799)* mutant animals at 4°C. Error bars indicate the SEM from 6 biological replicates. A minimum of 800 animals were scored per time point. Wilcoxon signed-rank test was used for statistical analysis; p = 0.03. (**B**) Graphical model of IRE-1 activation in the cold. Cold exposure leads to increased protein misfolding and lipid disequilibrium in the ER. These two stressors trigger the activation of IRE-1, which promotes

the downstream processing of *xbp-1u* to *xbp-1s* mRNA. The functional XBP-1 transcription factor enters the nucleus to promote transcription of specific genes, including those facilitating cold survival. Created with BioRender.com.

SUPPLEMENTARY FIGURES

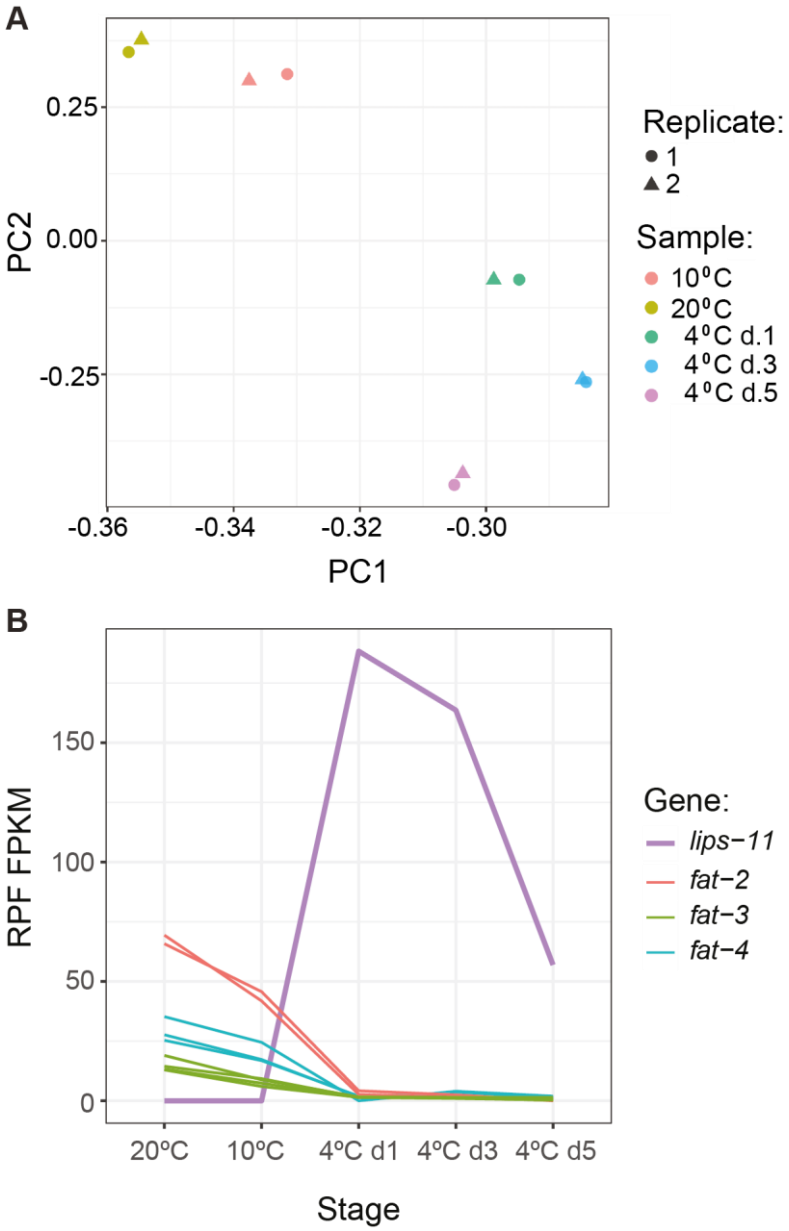

Figure 2 – figure supplement 1.

(**A**) PCA plot of ribosome profiling samples and replicates based on transcript RFP FPKM. Note co-clustering of replicates and temperatures. (**B**) Changes in translation for selected genes as a function of temperature changes and exposure.

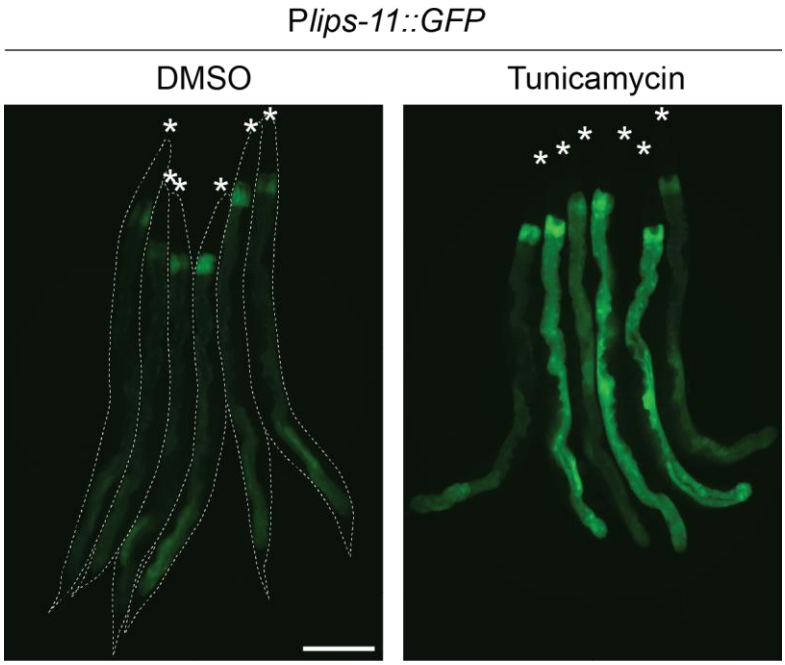

Figure 3 – figure supplement 1.

Micrographs taken of several bundled P*lips-11::GFP* reporter animals after 6 hours of treatment with DMSO or tunicamycin. DMSO treated control animals are outlined in the left panel and the head of all separate animals are indicated with asterisks. The scale bar = 200 µm.

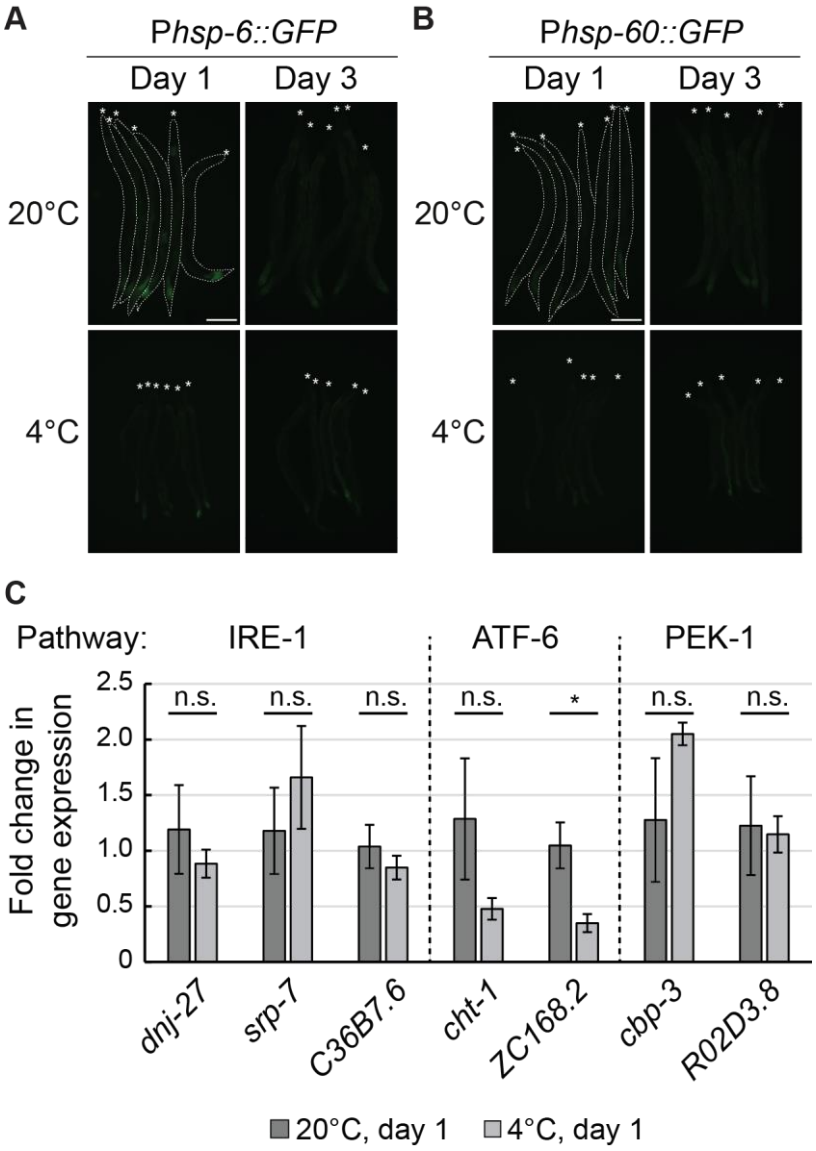

Figure 4 – figure supplement 1.

(**A**) Micrographs taken of several bundled P*hsp-6::GFP* UPR^{mito} reporter animals, taken at the indicated time and temperature. Animals are outlined in the 20°C control panel for day 1 and the head of all separate animals are indicated with asterisks. The scale bar = 200 µm. (**B**) Micrographs taken of several bundled P*hsp-60::GFP* UPR^{mito} reporter animals, taken at the indicated time and temperature. Animals are outlined in the 20°C control panel for day 1 and the head of all separate animals are indicated with asterisks. The scale bar = 200 µm. (**C**) RT-qPCR analysis of fold change in mRNA levels for known UPR^{ER} target genes after one day at 4ºC, relative to one day at 20ºC. Dashed lines separate genes that are regulated by different

pathways (IRE-1, ATF-6, and PEK-1). Error bars indicate the SEM of three biological replicates. Unpaired two-sided t-test was used for statistical analysis. ns: $p > 0.05$, *: $p < 0.05$.

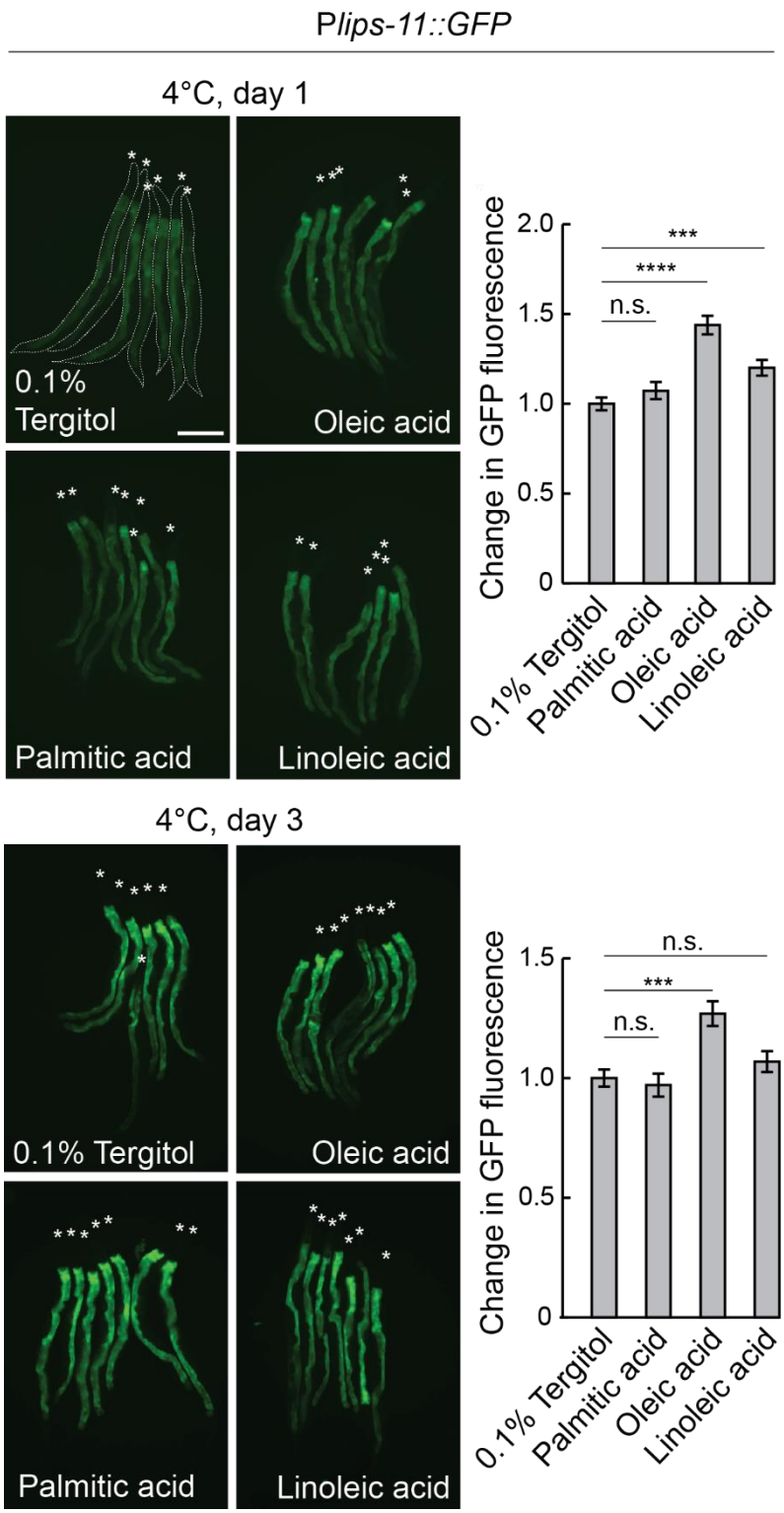

Figure 6 – figure supplement 1.

Left: Micrographs taken after one or three days at 4ºC of several bundled P*lips-11::GFP* reporter animals on a 0.1% Tergitol mock diet or a 0.8 mM oleic acid, 0.8 mM palmitic acid, or 0.8 mM linoleic acid supplemented diet. Mock treated animals after one day at 4°C are

outlined and the head of all separate animals are indicated with asterisks. The scale bar = 200 µm. Right: the corresponding quantification of intestinal GFP fluorescence after one or three days at 4ºC on the different fatty acid supplemented diets, relative to the mock diet. GFP fluorescence was analyzed from 21 to 31 animals per condition. Error bars indicate the SEM. Unpaired two-sided t-test was used for statistical analysis. N.s.: $p > 0.05$, ***: $p < 0.001$, ****: $p < 0.0001$.

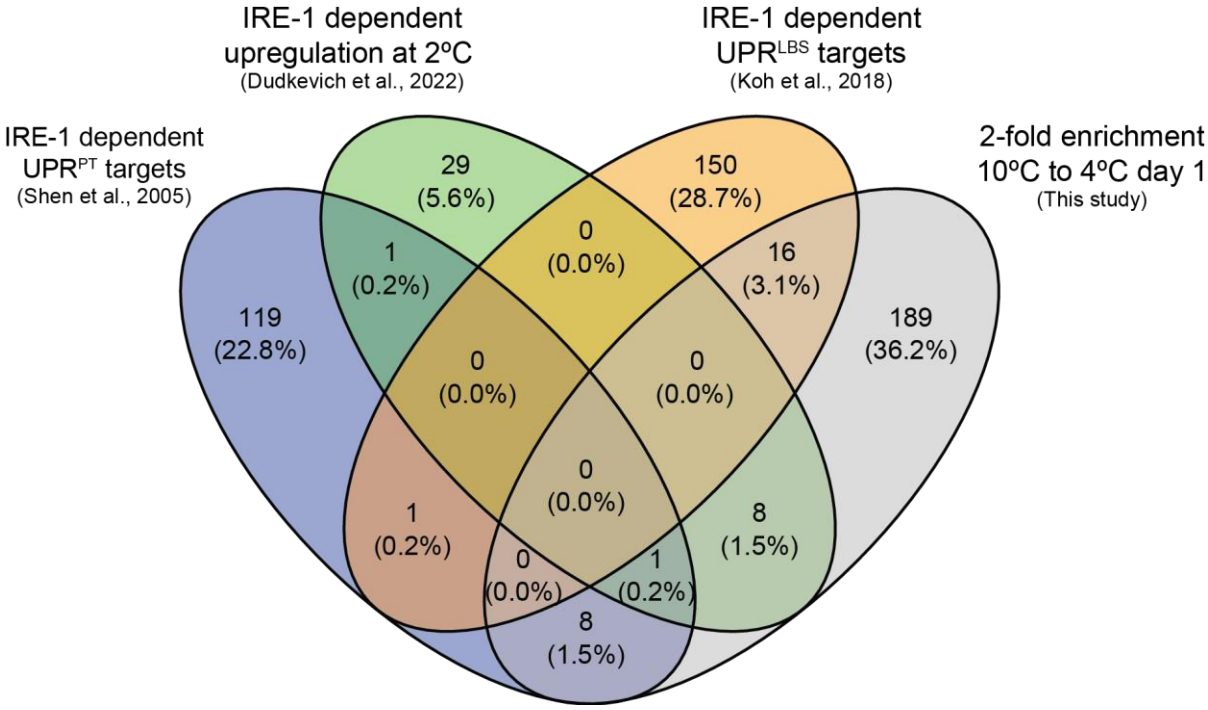

Figure 7 – figure supplement 1.

Four-way Venn diagram depicting the overlap between genes with a minimum 2-fold enrichment (10ºC to 4ºC day 1) and previously reported IRE-1 responsive genes that are upregulated either during the UPR^{PT} (Shen et al., 2005), upon shifting animals from 15ºC to 2ºC (Dudkevich et al., 2022), or during the UPR^{LBS} (Koh et al., 2018).

SUPPLEMENTARY FILE LEGENDS

Supplementary file 1.

Total RNA-seq data of wild-type animals kept at the different indicated temperatures.

Supplementary file 2.

Ribo-seq data of wild-type animals kept at the different indicated temperatures.

Supplementary file 3.

List of genes highlighted in Figure 2A in red.

Supplementary file 4.

IRE-1 responsive genes from published datasets used to generate the Venn diagram in Figure 7 – figure supplement 1. The IRE-1 dependent cold genes were selected from Table S2 and Table S3 from Dudkevich and colleagues (Dudkevich et al., 2022), genes were selected if they were in an upregulated cluster in wild-type animals at 2ºC and absent from upregulated clusters in *ire-1(ok799)* mutants.

Supplementary file 5.

Supplemental tables describing the *C. elegans* strains (5A) and oligos (5B) used in this study.